DTIC FILE COPY

(2)

SECURITY CLASSIFICATION OF THIS PAGE

REPORT DOCUMENTATION PAGE

1a. REPORT SECURITY CLASSIFICATION	1b. RESTRICTIVE MARKINGS: None
	3. DISTRIBUTION/AVAILABILITY OF REPORT: Unlimited
AD-A199 247	5. MONITORING ORGANIZATION REPORT NUMBER(S)
Interium Technical Report #21	
6a. NAME OF PERFORMING ORGANIZATION: Department of Chemistry	6b. OFFICE SYMBOL (If applicable):
7a. NAME OF MONITORING ORGANIZATION: Office of Naval Research	
6c. ADDRESS (City, State, and ZIP Code): Massachusetts Institute of Technology, 77 Mass. Avenue, Bldg. 6-335, Cambridge, MA 02139	7b. ADDRESS (City, State, and ZIP Code): Chemistry Division, 800 N. Quincy Street, Arlington, VA 22217
8a. NAME OF FUNDING/SPONSORING ORGANIZATION: Office of Naval Research	8b. OFFICE SYMBOL (If applicable):
9. PROCUREMENT INSTRUMENT IDENTIFICATION NUMBER: N00014-84-K-0553	
8c. ADDRESS (City, State, and ZIP Code): Chemistry division, 800 N. Quincy Street, Arlington, VA 22217	10. SOURCE OF FUNDING NUMBERS: PROGRAM ELEMENT NO. / PROJECT NO. / TASK NO. 051-579 / WORK UNIT ACCESSION NO.

11. TITLE (Include Security Classification): Ruthemium Oxide-Based Microelectrochemical Devices: Electrochem. Behavior of the Oxide Formed by Reduction of RuO_4^{2-}

12. PERSONAL AUTHOR(S): D.F. Lyons, M.O. Schloh, J.J. Hickman and M.S. Wrighton

13a. TYPE OF REPORT	13b. TIME COVERED	14. DATE OF REPORT (Year, Month, Day)	15. PAGE COUNT
technical interim	FROM _____ TO _____	August 17 1988	39

16. SUPPLEMENTARY NOTATION: Prepared for Publication in Journal of Physical Chemistry

17. COSATI CODES			18. SUBJECT TERMS (Continue on reverse if necessary and identify by block number)
FIELD	GROUP	SUB-GROUP	microelectrodes, ruthenium-oxide, transistors

19. ABSTRACT (Continue on reverse if necessary and identify by block number)

See Attached Sheet

20. DISTRIBUTION/AVAILABILITY OF ABSTRACT	21. ABSTRACT SECURITY CLASSIFICATION
☐ UNCLASSIFIED/UNLIMITED ☐ SAME AS RPT. ☐ DTIC USERS	Unlimited
22a. NAME OF RESPONSIBLE INDIVIDUAL: Mark S. Wrighton	22b. TELEPHONE (Include Area Code): 617-253-1597 / 22c. OFFICE SYMBOL

DD FORM 1473, 84 MAR — 83 APR edition may be used until exhausted. All other editions are obsolete. — SECURITY CLASSIFICATION OF THIS PAGE

Abstract

Properties of macroscopic electrodes and arrays of closely spaced (1.2 μm) Au microelectrodes (~2 μm wide x 50 μm long x 0.1 μm high) coated with the oxide (RuO_x) derived from reduction of RuO_4^{2-} in 1 M NaOH are reported. XPS data show RuO_x consists of a mixture of Ru oxidation states with significant amounts of Ru^{IV}. RuO_x exhibits a well-defined cyclic voltammetric wave centered at E_{redox} = 0.0 V vs. SSCE in pH 7.0 solution. The position, shape and area of the wave are insensitive to electrolyte composition, e.g. buffered solutions of LiCl, NaCl, $CaCl_2$, $(NH_4)Cl$, $Na(ClO_4)$ Na(OAc), Na(OTs), or Na(phosphate). A pH dependence of 71 mV/pH unit from pH = 2 to pH = 14 is found for the position of this wave. UV-vis spectroelectrochemistry shows four broad absorption bands in reduced RuO_x. Oxidation increases absorbance across the entire visible spectrum, but the data suggest that only a fraction of the RuO_x is electroactive. Electrical connection of microelectrodes by RuO_x was verified by cyclic voltammetry. The steady state resistance of RuO_x films has been measured as a function of potential and was typically found to vary from $\sim 10^9$ ohms for the reduced film to $\sim 10^6$ ohms for the film at potentials ~100 mV positive of E_{redox}. At more positive potentials, film resistance increases. The minimum resistance corresponds to a resistivity of approximately 300 ohm-cm. The potential at which minimum resistance occurs has a 71 mV/pH unit dependence, but the magnitude of the resistance is not affected by pH. RuO_x-based microelectrochemical transistors can amplify power, but the maxium frequency (~0.1 Hz) is limited by the slow electrochemistry of RuO_x films. A pair of microelectrodes connected by RuO_x functions as a pH-sensitive microelectrochemical transistor and detection of a change of pH in a flowing stream was demonstrated. A model is proposed for the structure of RuO_x consisting of relatively ordered domains surrounded by oxoruthenium moieties.

Office of Naval Research

Contract N00014-84-K-0553

Task No. 051-579

Technical Report #21

Ruthenium Oxide-Based Microelectrochemical Devices: Electrochemical Behavior of the Oxide Formed by Reduction of RuO_4^{2-}

by

Djonald F. Lyons, Martin O. Schloh, James J. Hickman

and Mark S. Wrighton

Department of Chemistry
Massachusetts Institute of Technology
Cambridge, MA 02139

Prepared for Publication in

Journal of Physical Chemistry

August 15, 1988

[Prepared for Publication in the

Journal of Physical Chemistry]

RUTHENIUM OXIDE-BASED MICROELECTROCHEMICAL DEVICES: ELECTROCHEMICAL BEHAVIOR OF THE OXIDE FORMED BY REDUCTION OF RuO_4^{2-}

Donald F. Lyons, Martin O. Schloh, James J. Hickman,

and Mark S. Wrighton*

Department of Chemistry

Massachusetts Institute of Technology

Cambridge, Massachusetts 02139

*Address all correspondence to this author.

Abstract

Properties of macroscopic electrodes and arrays of closely spaced (1.2 μm) Au microelectrodes (~2 μm wide x 50 μm long x 0.1 μm high) coated with the oxide (RuO_x) derived from reduction of RuO_4^{2-} in 1 M NaOH are reported. XPS data show RuO_x consists of a mixture of Ru oxidation states with significant amounts of Ru^{IV}. RuO_x exhibits a well-defined cyclic voltammetric wave centered at E_{redox} = 0.0 V vs. SSCE in pH 7.0 solution. The position, shape and area of the wave are insensitive to electrolyte composition, e.g. buffered solutions of LiCl, NaCl, $CaCl_2$, $(NH_4)Cl$, $Na(ClO_4)$ Na(OAc), Na(OTs), or Na(phosphate). A pH dependence of 71 mV/pH unit from pH = 2 to pH = 14 is found for the position of this wave. UV-vis spectroelectrochemistry shows four broad absorption bands in reduced RuO_x. Oxidation increases absorbance across the entire visible spectrum, but the data suggest that only a fraction of the RuO_x is electroactive. Electrical connection of microelectrodes by RuO_x was verified by cyclic voltammetry. The steady state resistance of RuO_x films has been measured as a function of potential and was typically found to vary from ~10^9 ohms for the reduced film to ~10^6 ohms for the film at potentials ~100 mV positive of E_{redox}. At more positive potentials, film resistance increases. The minimum resistance corresponds to a resistivity of approximately 300 ohm-cm. The potential at which minimum resistance occurs has a 71 mV/pH unit dependence, but the magnitude of the resistance is not affected by pH. RuO_x-based microelectrochemical transistors can amplify power, but the maxium frequency (~0.1 Hz) is limited by the slow electrochemistry of RuO_x films. A pair of microelectrodes connected by RuO_x functions as a pH-sensitive microelectrochemical transistor and detection of a change of pH in a flowing stream was demonstrated. A model is proposed for the structure of RuO_x consisting of relatively ordered domains surrounded by oxoruthenium moieties.

We wish to report the characterization of an electrochemically deposited ruthenium oxide, RuO_x, and its use as the active material in a microelectrochemical transistor. In connection with microelectrochemical devices RuO_x is unique because it is useful over a wide pH range (2-14) and its "conductivity" vs. potential is similar to that of a conventional redox polymer showing a well-defined peak at a potential that depends on pH. Ruthenium oxides are currently of immense importance as electrocatalysts and have been studied extensively.[1] Ruthenium oxides formed electrochemically from a solution species, however, have not been investigated in depth. Anderson and Warren described a route to an electrodeposited ruthenium oxide by oxidation of $(\eta^6\text{-}C_6H_6)Ru(OH_2)_3^{2+}$,[2] and Lam, Johnson and Lee reported the formation of black precipitate upon reduction of RuO_4^{2-},[3] and in each investigation the electrochemical behavior of the RuO_x film was described. We have examined the oxide formed upon reduction of RuO_4^{2-} in order to understand the behavior of ruthenium oxide-based microelectrochemical transistors. In particular, we report the potential dependence of conductivity and the pH dependence of the electrochemical response. Additionally, aspects of morphology, composition, and spectroelectrochemistry are reported. Throughout this paper, the oxide derived from reduction of RuO_4^{2-} will be referred to as RuO_x.

Closely spaced (1.2 μm) microelectrodes (~2 μm wide by ~50 μm long by ~0.1 μm high) are useful for studying the potential dependence of the conductivity of RuO_x. Such conductivity studies of $Ni(OH)_2$[4] and WO_3[5] films as well of as the organic conducting polymers polyaniline,[6] polypyrrole,[7] and poly(3-methylthiophene)[8] have been accomplished on such microelectrodes. Microelectrochemical transistors based on these materials have already been demonstrated.[4-8] It is important to note that materials with a conductivity that varies with the applied electrochemical potential are necessary for the

operation of microelectrochemical transistors. Materials that exhibit a constant conductivity at all potentials (for example, the oxide formed upon pyrolysis of $RuCl_3$)[9] can not be used as the basis for an electrochemical device. We will demonstrate that RuO_x does indeed exhibit a potential-dependent conductivity and that pH sensitive microelectrochemical transistors can be constructed with RuO_x.

Scheme I illustrates the operation of a microelectrochemical device based on RuO_x. A RuO_x film covers and electrically connects two adjacent microelectrodes. V_G, the gate potential, establishes the state of charge of the RuO_x film. The gate current, I_G, is associated with the faradaic processes that accompany changes in the state of charge of RuO_x driven by changes in V_G. A small potential difference, V_D, or the drain potential, can be maintained between the two microelectrodes The more negative electrode is called the source and more positive the drain, in analogy to transistor nomenclature. The current flowing between the microelectrodes is the drain current, I_D, and reflects the conductivity of the RuO_x film for a particular V_G. When V_G equals V_G^1, where RuO_x is insulating, there is no current flowing in the drain circuit: $I_D = 0$. When V_G is moved to a potential at which RuO_x is partially oxidized, V_G^2, there is current in the drain circuit, $I_D > 0$, for a finite V_D, and this is the maximum I_D obtained from a RuO_x-based device When V_G is moved to a potential at which RuO_x is fully oxidized, V_G^3, again $V_D > 0$, but it will be less than that obtained at V_G^2. Microelectrochemical transistors resemble solid-state transistors, but a key difference is that in a solid state device I_G is simply a capacitive current,[10] rather than a faradaic current associated with actual electrochemistry. A second significant difference for the RuO_x-based device is that the I_D-V_G characteristic shows a well-defined maximum at a V_G that depends on the pH of the electrolyte to which the device is exposed.

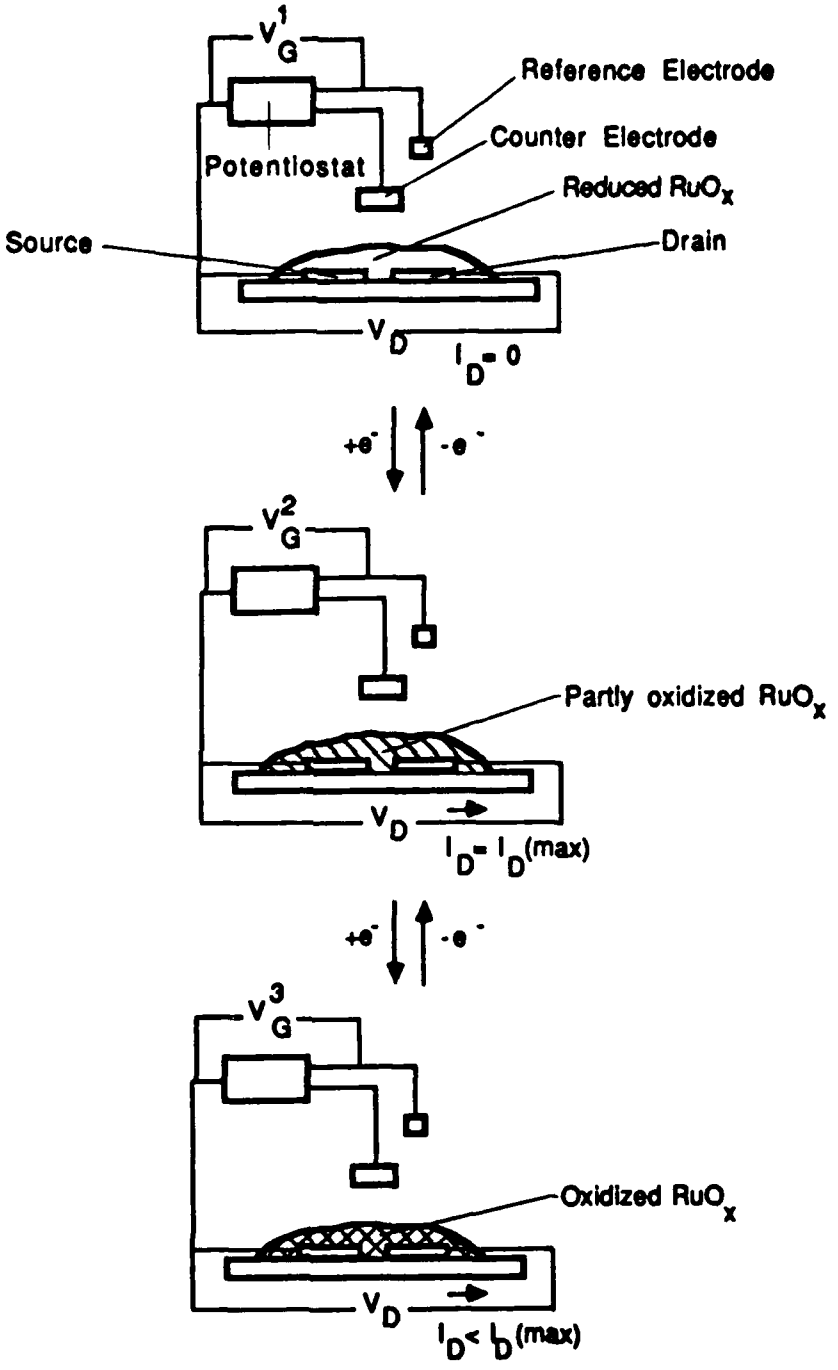

Scheme I. RuO_x-based microelectrochemical transistor.

Experimental

$K_2RuO_4 \cdot 2H_2O$ (Alfa) was used as received and stored in a controlled atmosphere chamber under N_2. All other chemicals and materials including the SnO_2-coated glass were used as received from commercial sources.

Electrochemical instrumentation consisted of Pine Instruments RDE 4 Bipotentiostats with Kipp and Zonen BD 91 XYY'T recorders for microelectrode experiments, and an ECO 551 potentiostat controlled by a PAR 175 programmer with a Houston Instruments 2000 XY recorder for macroscopic electrode experiments. A SSCE (sodium chloride-saturated calomel electrode) was used as reference and all potentials quoted are vs. SSCE.

Spectroelectrochemistry was monitored on a Hewlett Packard 8451A rapid-scan spectrometer. Thickness measurements were made with a Tencor Instruments Alpha Step 100 surface profiler with a 12.5 μm radius stylus and a tracking force of 5 mg. Flowing streams were produced and delivered to microelectrodes using the pumps of a Hewlett Packard 1084-B high pressure liquid chromatograph. Scanning electron micrographs were obtained on a Hitachi S 800 instrument . Auger electron spectra were obtained on a Physical Electronics 660 Scanning Auger Microprobe. X-ray photoelectron spectra were obtained on a Physical Electronics 584 spectrometer or on a Surface Science Laboratories spectrometer SSX-100 and signals were referenced to C 1s at 284.6 eV.

Microelectrodes used in these experiments were of a design previously described.[4-8] Each chip consists of an array of eight parallel Au or Pt microelectrodes on an insulating layer of Si_3N_4, surrounded by macroscopic contact pads. Each microelectrode was 50 μm long, 2.4 μm wide, and 0.1 μm thick, and electrode separation was 1.2 μm. Insulation was provided by either an additional layer of Si_3N_4 or epoxy. Cleaning and testing of microelectrodes

followed previously published procedures.[6-8]

RuO_x deposition was carried out from a freshly prepared 5 mM K_2RuO_4/1 M NaOH solution. A two-compartment cell was used with the counter electrode separated from the working and reference electrodes. Cycling a macroscopic working electrode at 100 mV/s between -0.2 and -0.8 V leads to the growth of a film of RuO_x associated with a cyclic voltammetry wave centered at -0.54 V. Gentle washing of the electrode after RuO_x deposition removes loosely bound particles of RuO_x, but does not affect the cyclic voltammetric signal. Deposition of RuO_x onto microelectrode arrays was performed in the same manner as onto macroscopic electrodes. Microelectrodes which were to be left underivatized were held at +0.2 V during the deposition procedure.

Results and Discussion

Characterization of Electrochemically Deposited RuO_x on Macroscopic Electrodes and Microelectrode Arrays. Deposition of RuO_x films is based on the literature procedure [3] Electrode composition does not seem to be important as we have successfully derivatized glassy carbon, SnO_2, Au, and Pt electrodes Films of up to 0.5 μm thick have been prepared as measured by profilometry and SEM data Films of this thickness are fragile and can be removed by vigorous washing, but 0.1 μm thick films are durable. Figure 1 shows a scanning electron micrograph of a RuO_x film deposited on Pt. The RuO_x appears granular and is also punctuated with larger holes which expose more oxide underneath. Unlike the oxide formed on Ru electrodes[11] or that formed via pyrolysis of $RuCl_3$,[9] both of which have a fairly compact morphology, RuO_x appears porous and nonuniform.

X-ray photoelectron spectrosopy of RuO_x films withdrawn from a pH 7.5 Na phosphate solution at -0.5 V shows a broad Ru $3d_{5/2}$ signal at 282.0 eV which apparently indicates a mixture of Ru oxidation states.[12] The binding energy of RuO_x is very close to that reported for RuO_2[12b] indicating that Ru is present as at least the +4 oxidation state RuO_x-derivatized electrodes withdrawn from the pH 7.5 solution at 0.0 and 0.35 V give almost identical XPS results. Apparently some degree of surface oxidation of RuO_x may occur as the electrode is removed from solution and transferred to the spectrometer which prevents a clear distinction between the binding energies of the three RuO_x oxidation states. An Auger electron element map of a microelectrode array in which the central four electrodes had been derivatized and the other four electrodes were kept underivatized reveals that Ru is present on the central electrodes and absent on the outer electrodes, Figure 2. Interestingly, Ru signals were seen on the area

surrounding the electrode array. This is consistent with an EC mechanism for oxide deposition in which RuO_4^{2-} is reduced to a soluble Ru^{IV} species which subsequently decomposes to an insoluble ruthenium oxide.[3] The small size of individual electrodes permits the soluble Ru^{IV} species to diffuse away and decompose on electroinactive areas. The Auger map in Figure 2 establishes that it is possible to selectively modify the microelectrode array by controlling the potential of electrodes to remain free of RuO_x.

The cyclic voltammetry of the RuO_x film is depicted in Figure 3 and shows a wave centered at 0.0 V at pH 7. The wave is broad and has been attributed to the $Ru^{IV/III}$ couple.[3] Further oxidation, which begins at +0.35 V in pH 7.0 solution, is assigned to the $Ru^{VI/IV}$ couple.[3] At more positive potentials, oxidation process overlaps H_2O oxidation to give O_2 evolution. Cycling RuO_x to the potential of O_2 evolution results in gradual film dissolution and obvious loss of electroactivity. However, the film is remarkably durable as long as the electrode potential is not moved more than 0 3 V more positive than the peak of the cyclic voltammetry wave: in one experiment a RuO_x-derivatized electrode was cycled for 18 h between +0.3 and -0.5 V in pH 7.5 solution with less than 5% loss in the area of the voltammogram for RuO_x. At potentials negative of the $Ru^{IV/III}$ wave, the RuO_x film shows no faradaic activity, but H_2 evolution occurs A slight capacitive current is observed between the H_2 evolution and $Ru^{IV/III}$ wave indicating that the film is not totally insulating in this potential regime (vide infra). Prolonged H_2 evolution (~15 min at 5 mA/cm^2) does not affect the $Ru^{IV/III}$ voltammogram.

The voltammetry of the electrodeposited RuO_x film resembles that of the film produced upon oxidation of $(\eta^6\text{-}C_6H_6)Ru(OH_2)_3^{2+}$.[2] In contrast, ruthenium oxide

films produced by pyrolysis of $RuCl_3$[13] or by Ru anodization[10,14,15] exhibit large, apparently capacitive currents with only small peaks in the current-voltage scans. Apparently, RuO_x films deposited from RuO_4^{2-} in solution behave in a manner which is very similar to conventional redox polymers.[16] The integral of the cyclic voltammogram, coupled with measurements of thickness, show that the oxidation/reduction associated with the wave at 0.0 V at pH = 7.0 involves >100 C/cm^3. This is similar to the charge density for conventional redox polymers.[16] Ruthenium oxides formed by pyrolysis or anodization show electrochemical behavior[13-15] which resembles porous metallic electrodes with high conductivity and apparently capacitive behavior.[17] It should be noted though, that the electrodeposited RuO_x films described here are much better conductors than simple redox polymers such as those derived from viologens.[18]

RuO_x electrochemistry is pH dependent and in unbuffered solutions the voltammetric waves become poorly defined. The average of the anodic and cathodic peaks for $Ru^{IV/III}$ varies by 71 mV/pH unit from pH 2 to pH 14 as shown in Figure 4. This relationship indicates that slightly more than one proton is lost from the film for every electron that is withdrawn (approximately 7 H^+ per 6 e^-). The pH dependence is similar for both NaCl and $NaNO_3$ supporting electrolytes. This type of non-Nernstian pH dependence has been observed in the voltammetry of several hydrous metal oxides (Ni,[19] Ir,[20] Rh,[21] Au[22], Pd[23]) as well as in thermally prepared RuO_2.[24] This effect is usually attributed to the acid-base properties of the oxides. For example, proton loss from coordinated H_2O molecules may occur upon oxidation due to the higher positive charge on the central metal atoms.[25]

We have studied cation and anion effects on the RuO_x electrochemistry. 0.05 M buffer, 1.0 M electrolyte solutions were prepared. For cations, a pH 4.0 NaOAc buffer was used with LiCl, NaCl, $CaCl_2$, or NH_4Cl as the supporting

electrolyte. For anions, a pH 7.0 Na^+ phosphate buffer was used with NaCl, $NaClO_4$, or Na(tosylate) as supporting electrolyte. Additionally, a pH 7.5, 0.5 M Na^+ phosphate solution was examined. No change in the shape, area or position of the RuO_x voltammogram (5 mV/s) for a fixed pH is found. These results indicate that, in general, RuO_x is insensitive to electrolyte composition as long as the solution pH is maintained by a buffer.

The relationship of the voltammetric peak current to the scan rate is a widely used technique to determine the charge transport properties of chemically modified electrodes.[16] We have examined the peak current/scan rate behavior of Pt/RuO_x electrodes while recognizing that this method may be affected by uncompensated ohmic drop through the film, by the rate of electron exchange between the film and the electrode, or by localized pH changes at high scan rates.[26] The data, Figure 5, show a qualitative increase in the apparent D_{CT} of the RuO_x at low pH's. At low scan rates no pH effect is observed on peak current, but the higher scan rates reveal slow oxidation in basic solutions. AC impedance results on anodically and thermally grown ruthenium oxides were interpreted as showing proton motion to be important in the conduction mechanism,[27] but this does not provide insight into why low pH results in faster oxidation.

RuO_x exhibits electrochromism in the UV-Vis region. Figure 6 shows spectroelectrochemistry of RuO_x-derivatized SnO_2 electrodes. The reduced RuO_x exhibits five absorption bands centered at 332, 374, 440, 548, 738 nm. Changing the electrode potential to more positive potentials increases film absorption across the entire spectrum. The UV-Vis spectrum appears to show no clearly defined new bands upon oxidation of the RuO_x film. However, the difference UV-Vis does show broad new bands which grow in at 402, 454, 580 and

800 nm. Similar electrochromic behavior is found in solutions with a pH of 4.3 or 9.6. The fact that the actual UV-Vis shows no well-defined peaks is likely a reflection of the fact that only a fraction of the RuO_x actually undergoes oxidation/reduction.

We have characterized RuO_x on microelectrode arrays by cyclic voltammetry. The cyclic voltammetry of four adjacent Au microelectrodes derivatized with RuO_x is shown in Figure 7. The area of the cyclic voltammogram of four electrodes driven together is essentially the same as those of the individual electrodes at 20 mV/s. This indicates that there is an electrical connection between the microelectrodes via RuO_x. If there were no connection, the area of the cyclic voltammogram of the four adjacent microelectrodes driven together would be the sum of the individual voltammograms. The cyclic voltammograms at 50 mV/s in Figure 7 do show evidence of sluggish charge transport through the RuO_x film, because the area of the cyclic voltametry when all four electrodes are driven together is larger than for any individual electrode. At very slow scan rates (<10 mV/s), all RuO_x accessible to one microelectrode is accessible to another RuO_x-connected microelectrode. Similar behavior has been reported for WO_3- and $Ni(OH)_2$-derivatized microelectrode arrays.[4,5]

An important property of RuO_x is its resistance as a function of its potential. This property can be measured using two microelectrodes connected by a RuO_x film. In Figure 8, data are illustrated for RuO_x-connected microelectrodes at pH 7.5. Like previously characterized microelectrochemical devices, the change in resistance of RuO_x is associated with injection or withdrawal of charge in an electrochemical redox process. Measurement of the resistance entails bringing adjacent, RuO_x-connected electrodes to a given potential, V_G, waiting until redox equilibrium is established, and slowly

scanning the potential of one microelectrode by a small amount around V_G, while holding the adjacent electrode at V_G. With RuO_x-connected microelectrodes, measurements were made ~5 minutes after moving to a new V_G. Changes in resistance are observed by varying V_G through the region where redox processes occur. The current passing between the electrodes was measured and related to the resistance by Ohm's law.

The data in Figure 8 show that the resistance of RuO_x-connected microelectrodes varies by about three orders of magnitude, from $\sim 10^9$ ohms to $\sim 10^6$ ohms, as V_G is varied from -0.4 to 0.1 V, in pH 7.5 solution. At more positive potentials, film resistance actually increases by an order of magnitude. A similar resistance minimum has been observed for polyaniline-connected microelectrodes.[6] Such behavior is expected for conventional redox polymer-based microelectrode transistors.[28] The resistance minimum seen for RuO_x-connected microelectrodes is pH-dependent, and occurs ~100 mV positive of the peak in the cyclic voltammogram for RuO_x at a given pH. The measured resistance of different samples of RuO_x may vary from the data in Figure 8 by up to an order of magnitude, but the change in resistance for a particular sample never varies by more than three orders of magnitude. The resistance of RuO_x-connected microelectrodes in their most conducting state is much higher than for oxidized, conducting polymers derivatized onto microelectrodes.[6-8] In the insulating state, the resistance, as for WO_3[5] and $Ni(OH)_2$,[4] is lower than for the conducting organic polymers. The point is that the RuO_x shows only a $\sim 10^3$ change in conductivity and is always moderately conducting.

The resistance of RuO_x-connected microelectrodes per se is not especially meaningful information, since it can only be referenced to the resistance of

other redox-active electronic conductors derivatized on closely spaced microelectrodes of the same geometry. The resistivity, ρ, defined in equation (1), is a characteristic property of a material. In equation (1), l is the

$$R = \rho (l/A) \qquad (1)$$

length of a uniform conductor, and A is its cross sectional area. Assuming complete uniformity of RuO_x films, an approximate calculation of the resistivity can be made using the well-defined electrode geometry. For typical RuO_x-based devices, the 50 μm long microelectrodes are covered with a ~0.5 μm thick film. The length is taken to be the 1.2 μm spacing between microelectrodes. Calculations indicate that in the conducting state, the resistivity of electrochemically deposited RuO_x is 200-400 Ω-cm. This value is about equal to the resistivity of moderately doped single crystal semiconductors.[9] The sample to sample variability in resistance is probably a result of differences in film thickness rather than in resistivity. While the resistivity of RuO_x may be high for a "conducting" material, it is the potential dependence of the resistivity that leads to interesting consequences.

We believe that the electrochromism, voltammetry, conductivity maximum, and the large "background" conductivity of RuO_x can be explained by the following model. As depicted in Figure 9, the structure of RuO_x may consist of domains of relatively ordered ruthenium-oxygen networks surrounded by electroinactive oxoruthenium moieties. The UV-Vis absorption spectrum of RuO_x is a combination of absorption bands that are unaffected by the state of charge of the RuO_x from the oxoruthenium moieties, and bands that grow in upon oxidation from the ruthenium-oxygen networks. The redox process in RuO_x probably involves gain and loss of either protons or hydroxide groups from the ruthenium-oxygen network. It follows that while the electrolyte must be buffered to observe a well-defined

RuO_x voltammetric wave, the particular electrolyte composition has no effect on this wave. In addition, the absence of specific electrolyte effects on RuO_x voltammetry suggests that the electroactive networks are open and porous. Porous structures have been postulated for other hydrous metal oxides.[25] The magnitude of the resistivity of RuO_x implies some degree of electron delocalization and the existence of an electronic band. As RuO_x is oxidized or reduced this band is emptied or filled with electrons, and the partially filled band exhibits the highest conductivity. The heterogeneous structure of RuO_x limits the maximum conductivity by limiting electron mobility, but also introduces enough localized states, which can accept or donate electrons, to give a residual conductivity even when RuO_x is fully reduced.

Transistor Properties of RuO_x-connected Microelectrode Arrays. It has been established that redox materials that undergo large changes in resistance upon redox cycling can be used in transistor-like devices as the active switching material.[4-8] We have characterized the transistor properties of RuO_x-connected microelectrodes and established pH-dependent characteristics for an exceptionally wide range of pH.

When V_G is moved from V_G^1, where RuO_x is reduced, to V_G^2, where RuO_x is oxidized, and there is a potential difference V_D between two adjacent microelectrodes, I_D can be expected to go from close to zero to a finite value that depends on the magnitude of V_D. Figure 10 shows I_D vs. time when a RuO_x-based transistor is stepped from a V_G of -0.50 to +0.05 V and back in a pH 7.5 solution. With V_D = 100 mV, I_D changes reproducibly from zero at V_G = -0.50 V to 140 nA at V_G = 0.1 V. The limiting I_D for the 100 mV V_D implies a resistance of approximately 7.1×10^5 Ω at 0.1 V. The device takes approximately 10 seconds to achieve a steady state I_D with a 100 mV V_D. The

current spikes upon scan reversal are indicative of the charging current necessary to turn the device on and off. While the magnitude of I_D is limited at fixed V_D by the oxide resistance (and therefore V_G), the rate at which a particular I_D is attained is limited by the rate of faradaic processes associated with switching the RuO_x between different states of charge.

Evidence that RuO_x-based microelectrochemical transistors function as electrical power amplifiers is illustrated in Figure 11, which shows the magnitudes and relationships of V_G, I_G, and I_D for a slow triangular potential variation between -0.35 and +0.05 V in pH 7.0 buffer. While these relationships are best understood with respect to sinusoidally varying V_G, they can be interpreted with a triangular V_G as well. The average power amplification, A, is given by equation (2). For the data shown in Figure 11,

$$A = \frac{\text{average power in the drain circuit}}{\text{average power in the gate circuit}} \qquad (2)$$

A is equal to 1.8. In theory, at the same frequency and surface coverage, differences in the amplification ability of microelectrochemical transistors depend on the maximum conductivity of the materials used to connect adjacent microelectrodes. We find the observed amplification properties for devices prepared from redox active metal oxides and the conducting polymers accurately reflect the relative maximum conductivities of the materials. Power amplification is frequency dependent in that I_G increases with scan rate. Furthermore, at sufficiently high frequencies, limitations in rates of faradaic processes preclude complete turn on/turn off. The data in Figure 11 are obtained in the mHz frequency domain, while polyaniline-based microelectrochemical transistors with similar electrode geometry can amplify power at frequencies approaching 1 kHz.[29] The slow operating speed of RuO_x-microelectrochemical transistors is limited by the slow electrochemistry

of RuO_x films. At frequencies higher than ~0.1 Hz, RuO_x-based transistors do not amplify power, since $\underline{A} < 1$.

Figure 12 illustrates the steady state current voltage characteristics of a RuO_x-based microelectrochemical transistor. V_D is fixed at 100 mV and V_G is slowly scanned across the potential regime of interest. This RuO_x transistor was examined in three solutions of differing pH. We find essentially no difference in the maximum obtainable I_D from pH to pH. The potential at which I_D is a maximum occurs ~100 mV positive of the peak of the cyclic voltammogram in the same electrolyte and shifts by 71 mV/pH unit. Since I_D depends on the charge transport properties of RuO_x, these steady state data agree with the cyclic voltammetry results, at slow scan rates, on macroscopic electrodes. One might expect that upon increasing the scan rate in the I_D vs. V_G experiments, the charge transfer differences seen at macroscopic electrodes at high scan rates would become apparent. But because the maximum conductivity of RuO_x is so low, electrons can not diffuse all the way across the 1.4 μm gap between electrodes, and at scan rates >~50 mV/s the I_D vs. V_G curve looks more and more like a conventional cyclic voltammogram, exhibiting negative I_D on the return sweep. Microelectrode arrays with smaller electrode separations are currently under development in our group and will allow faster switching of RuO_x-based devices.[30]

The pH-dependent nature of the I_D vs. V_G data serves as the basis for a pH sensor, Figure 13. A RuO_x transistor was placed in the effluent stream of a HPLC and the pH of the stream varied from 5.5 to 7.3. V_G was fixed at 0.0V and V_D was set at 100 mV. At this V_G, RuO_x is poorly conducting in pH 5.5 solution, but is more conducting in pH 7.3 solution. Accordingly, I_D for this device is high in pH 7.3 and low in pH 5.5. The RuO_x-based device is

durable and maintains nearly constant I_D values over 5 h of operation. The stability of RuO_x over a wide pH range is a considerable improvement over WO_3 and $Ni(OH)_2$-based transistors[4,5] which fail in basic and acidic media, respectively

Conclusion

Reduction of RuO_4^{2-} in alkaline solution results in deposition of an oxide, RuO_x, exhibiting characteristics intermediate between "redox conducting" and "electronically conducting" materials. Like a conventional redox polymer, RuO_x shows a well-defined voltammetric wave and a conductivity maximum at a potential close to E_{redox}. But conductivity values obtained for RuO_x are much closer to those obtained for electronically conducting polymers and metal oxides. The E_{redox} of RuO_x is pH-sensitive, 71 mV/pH unit in the pH range 2-14. These properties allow the demonstration of a RuO_x-based microelectrochemical transistor which shows an I_D maximum in a I_D vs V_G plot and which is durable over a wide pH range (2-14).

Acknowledgements. We thank the Office of Naval Research and Defense Advanced Research Projects Agency for partial support of this research We also acknowledge support from the National Science Foundation Materials Research Laboratory at M.I.T.

References

1. Trasatti, S.; O'Grady, W.E., in Advances in Electrochemistry and Electrochemical Engineering; Gerischer, H., and Tobias, C.W., Eds.; Wiley: New York, 1981, vol. 12, p. 177.
2. Anderson, D.P; Warren, K. F. J. Electrochem. Soc., 1984, 131, 347.
3. Lam, K.W.; Johnson, K.E.; Lee, D.G. J. Electrochem. Soc., 1978, 125, 1069.
4. Natan, M.J.; Belanger, D.; Carpenter, M.K.; Wrighton, M.S. J. Phys. Chem., 1987, 91, 1834.
5. Natan, M.J.; Mallouk, T.E.; Wrighton, M.S. J. Phys. Chem., 1987, 91, 648.
6. Paul E.W.; Ricco, A.J.; Wrighton, M.S. J. Phys. Chem., 1985, 89, 1441.
7. Kittlesen, G.P.; White, H.S.; Wrighton, M.S. J. Amer. Chem. Soc., 1984, 106, 7389.
8. Thackeray, J.T.; White, H.S.; Wrighton, M.S. J. Phys. Chem., 1985, 89, 5133.
9. (a) Galizzioli, D.; Tantardini, F.; Transatti, S. J. Appl. Electrochem., 1975, 5, 203; (b) Pizzini, S.; Buzzana, G.; Mari, C.; Rossi, K.; Torcho, S. Mat. Res. Bull., 1972, 7, 449.
10. Sze, S. M. Physics of Semiconductor Devices, 2nd Edition; Wiley-Intersceince: New York, 1981.
11. Birss, V.; Myers, R.; Angerstein-Kozlowska, H.; Conway, B.E. J. Electrochem. Soc., 1984, 131, 1502.
12. (a) Kim, K.S.; Winograd, N. J. Catal., 1974, 35, 66; (b) Folkesson, B. Acta Chem. Scand. 1973, 27, 287.
13. (a) Trassati, S.; Buzzana, G. J. Electroanal. Chem., 1971, 29, App. 1.; (b) Galizzioli, D.; Tantardini, F.; Trasatti, S. J. Appl. Electrochem. 1974, 4, 57.

14. Hadzi-Jordanov, S.; Angerstein-Kozlowska, H.; Vukovic, M; Conway, B.E. J. Electrochem. Soc., 1978, 125, 1473.

15. Burke, L.D.; Mulcahy, J.K.; Venkatesan, S. J. Electroanal. Chem., 1977, 81, 339.

16. Murray, R.W. in Electroanalyical Chemistry, vol. 13; Bard, A.J., (Ed.), Marcel Dekker; New York, 1984, p. 191.

17. Feldberg, S.W. J. Amer. Chem. Soc., 1984, 106, 4671.

18. Lewis, T.J.; White, H.S.; Wrighton, M.S. J. Amer. Chem. Soc., 1984, 106, 6947.

19. Burke, L.D.; Twomey, T.A. M. J. Electronanal. Chem., 1984, 162, 101.

20. Burke, L.D.; Whelan, D.P. J. Electroanal. Chem., 1984, 162, 121.

21. Burke, L.D.; O'Sullivan, E.J.M. J. Electroanal. Chem., 1981, 129. 133.

22. Burke, L.D.; Lyons, M.E.; Whelan, D.P. J. Electroanal. Chem., 1982, 139, 131.

23. El Wakkad, S.E.S.; Shams El Din, A.M. J. Chem. Soc., 1954, 3094.

24. Burke, L.D.; Healy, J.F. J. Electroanal. Chem., 1981, 124, 327.

25. Burke, L.D.; Lyons, M.E.G. in Modern Aspects of Electrochemistry, No. 18; White, R.E., Bockris, J. O'M., Conway, B.E., (Eds.), Plenum: New York, 1986, p. 169.

26. Laviron, E. in Electroanalytical Chemistry, vol. 12, Bard, A.J., (Ed.), Marcel Dekker: New York, 1982, p. 53.

27. Rishpon, J.; Gottesfeld, S. J. Electrochem. Soc., 1984, 131, 1960.

28. Belanger, D.; Wrighton, M.S. Anal. Chem., 1987, 59, 1426.

29. Lofton, E.P.; Thackeray, J.W.; Wrighton, M.S. J. Phys. Chem., 1986, 90, 6080.

30. Jones, E.T.T.; Chyan, O.M.; Wrighton, M.S. J. Amer. Chem. Soc., 1987, 109, 5526.

Figure Captions

Figure 1. Scanning electron micrograph of RuO_x deposited onto a Pt electrode.

Figure 2. Scanning Auger map of ruthenium (top) and scanning electron micrograph (bottom) of a microelectrode array in which the central four electrodes are derivatized with RuO_x and the other four electrodes kept underivatized.

Figure 3. Cyclic voltammetry of glassy carbon/RuO_x in pH 7, 0.05 M sodium phosphate/0.3 M $NaNO_3$ solution. Scan rate: 10 mV/s.

Figure 4. Average position of cathodic and anodic current peaks from cyclic voltammetry of RuO_x as a function of pH. ●: C/RuO_x; ▲: Pt/RuO_x (both in 0.05 M buffer/1.0 M NaCl). X: Pt/RuO_x in 0.05 M buffer/1.0 M $NaNO_3$. Extrapolation of this line gives E_{redox} = +0.50 V vs. SSCE at pH = 0.

Figure 5. Peak anodic current for the RuO_x voltammetric wave at a Pt/RuO_x electrode. Solutions are 0.05 M buffer/1.0 M $NaNO_3$.

Figure 6. UV-Vis absorption (top) and difference (bottom) spectra for SnO_2/RuO_x. Electrode potentiostatted at -0.5, -0.4, -0.3, -0.2, -0.1, 0.0, 0.1, 0.2, and 0.3 V vs. SSCE.

Figure 7. Cyclic voltammograms at pH 7.5 of four individual adjacent RuO_x-connected microelectrodes and of the four driven together.

Figure 8. Resistance of RuO_x-connected microelectrodes as a function of V_G at pH 7.5. The data were obtained by scanning one electrode ±25 mV about V_G at 50 mV/s. The resistance is plotted on a logarithmic scale.

Figure 9. Proposed structure of RuO_x. Oxoruthenium moieties surround a porous ruthenium-oxygen domain.

Figure 10. I_D vs. time for a RuO_x-based transistor at pH 7.5 as V_G is stepped repetitively every 20 s from -0.50 to +0.05 V vs. SSCE and back. V_D = 100 mV.

Figure 11. Simultaneous measurement and phase relationship of V_G, I_G, and I_D for a RuO_x-based microelectrochemical transistor at pH 7.0 as V_G is repetitively swept linearly from -0.35 to +0.05 V vs. SSCE and back at a frequency of 0.1 Hz. V_D = 100 mV.

Figure 12. pH dependence of steady state I_D vs. V_G (at fixed V_D = 100 mV) for a RuO_x-based microelectrochemical transistor.

Figure 13. I_D vs. time for a RuO_x-based microelectrochemical transistor as the pH of a continuously flowing stream is varied from 5.5 to 7.3. V_G = 0.0 V vs. SSCE and V_D = 100 mV.

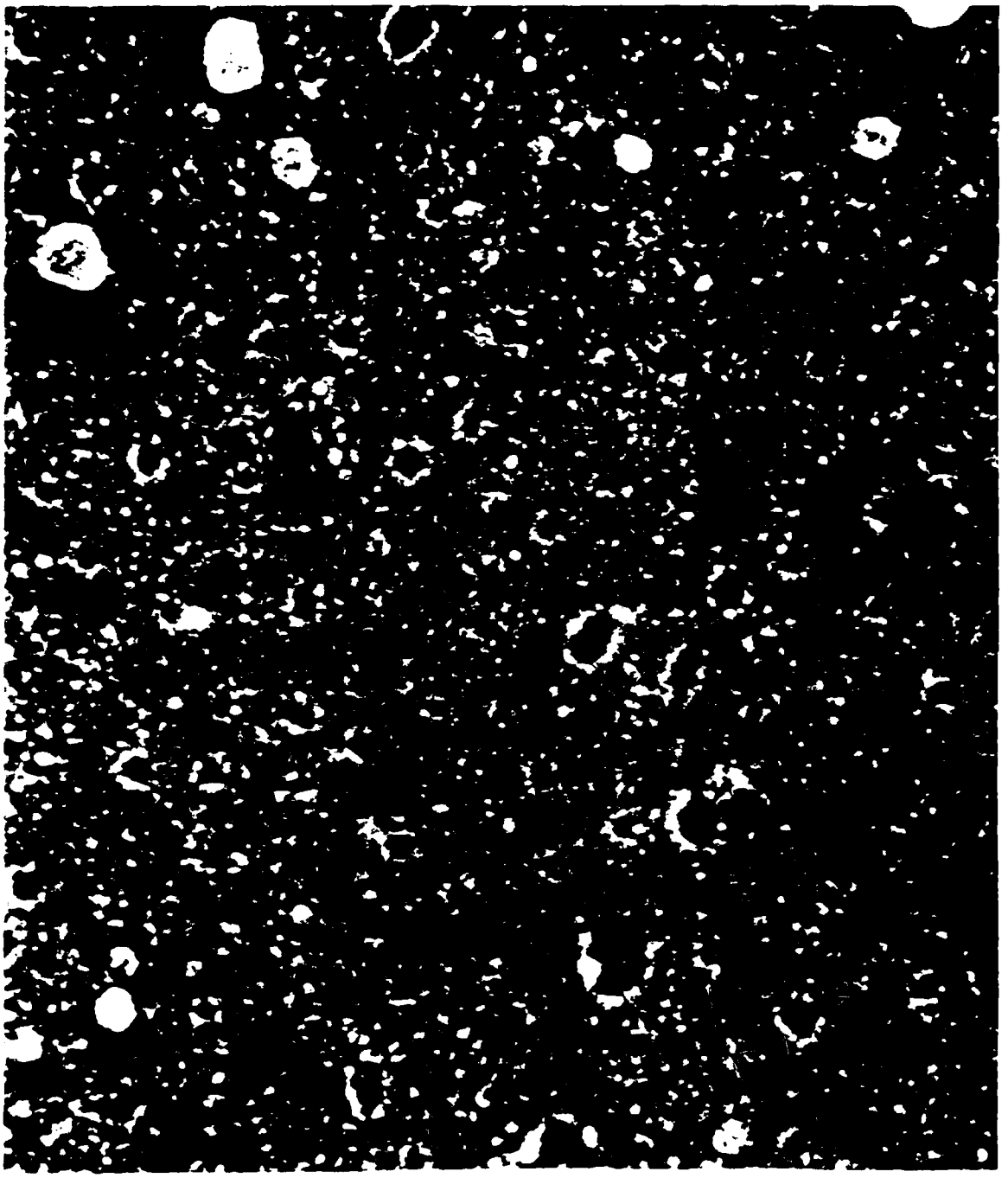

1600 nm


Ru
6.5 μm


SEM

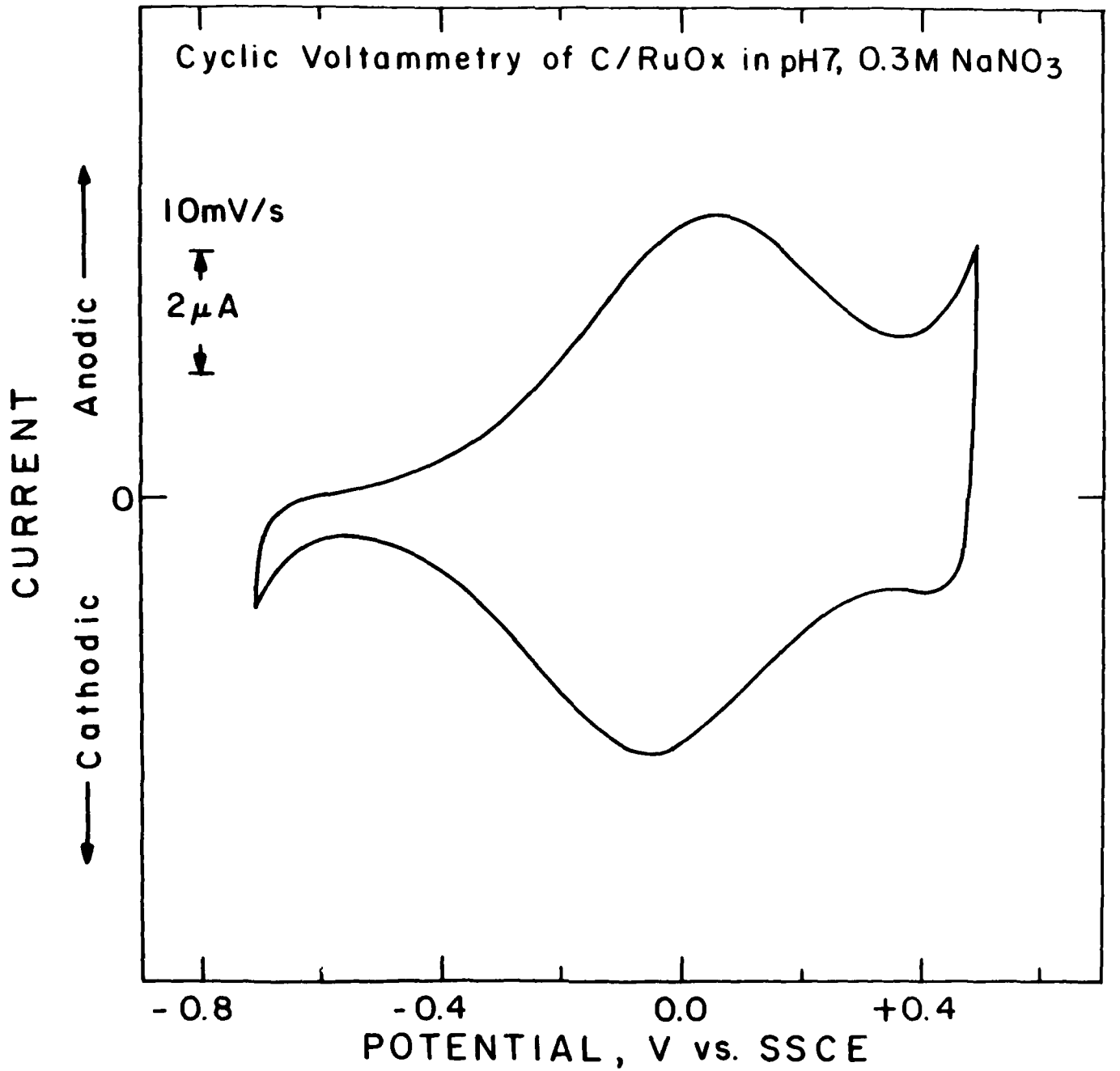
Cyclic Voltammetry of C/RuOx in pH7, 0.3M NaNO3
10mV/s
2μA
CURRENT
Anodic
Cathodic
0
-0.8
-0.4
0.0
+0.4
POTENTIAL, V vs. SSCE

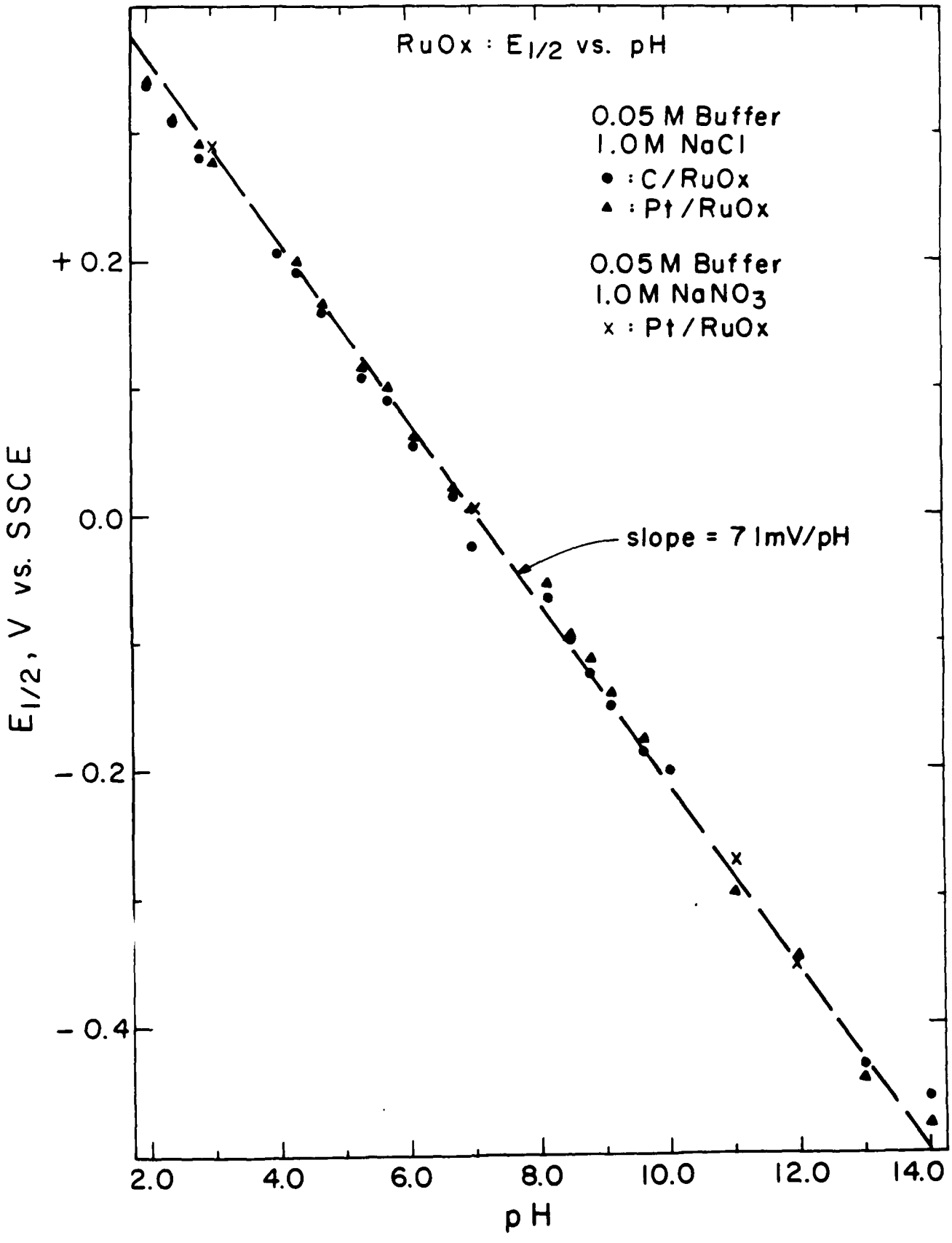
RuOx : E1/2 vs. pH
0.05 M Buffer
1.0 M NaCl
● : C/RuOx
▲ : Pt/RuOx
0.05 M Buffer
1.0 M NaNO3
x : Pt/RuOx
slope = 71 mV/pH
+0.2
0.0
−0.2
−0.4
E1/2, V vs. SSCE
2.0
4.0
6.0
8.0
10.0
12.0
14.0
pH

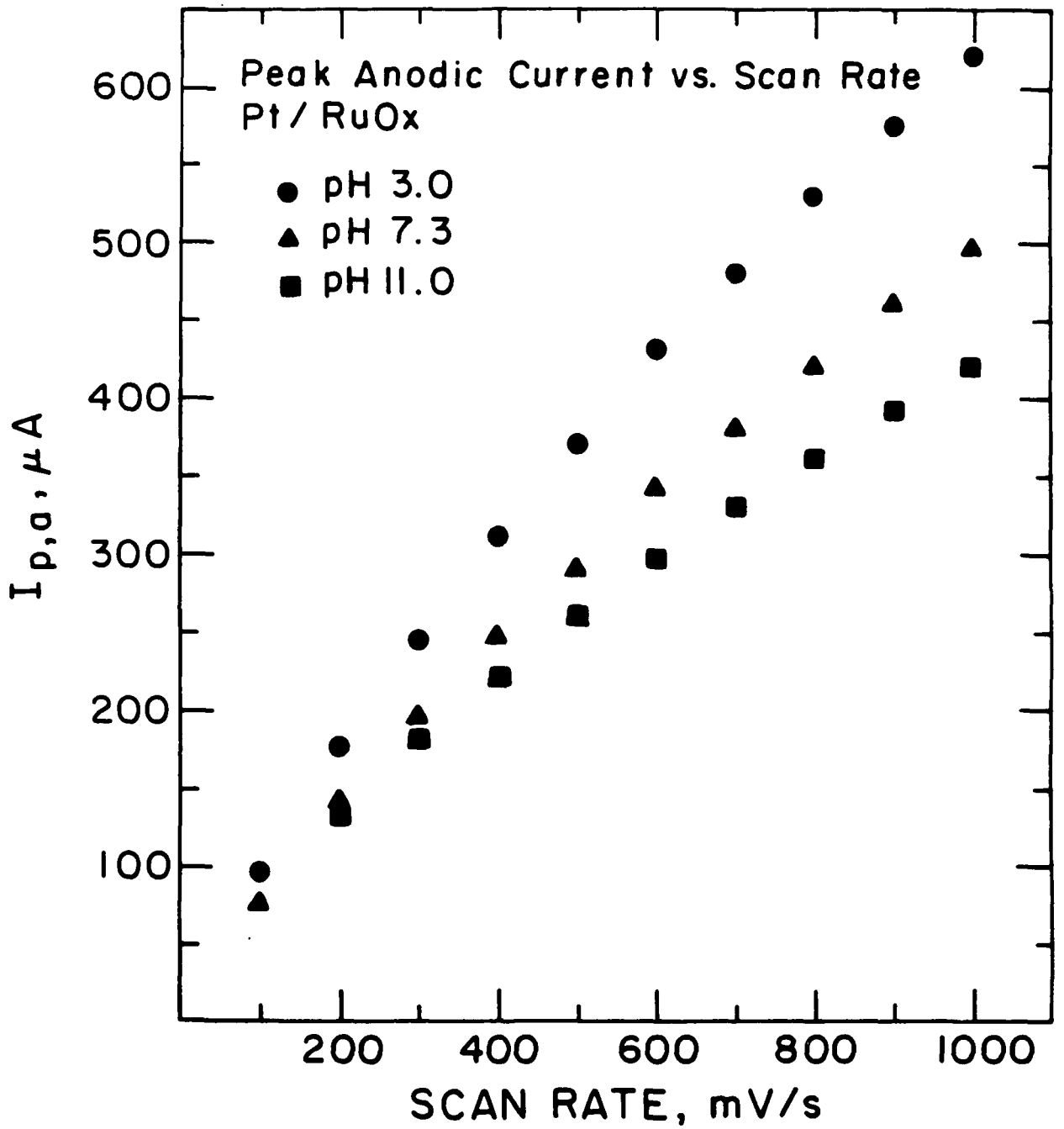
Peak Anodic Current vs. Scan Rate
Pt / RuOx
pH 3.0
pH 7.3
pH 11.0
600
500
400
300
200
100
$I_{p,a}$, μA
200
400
600
800
1000
SCAN RATE, mV/s

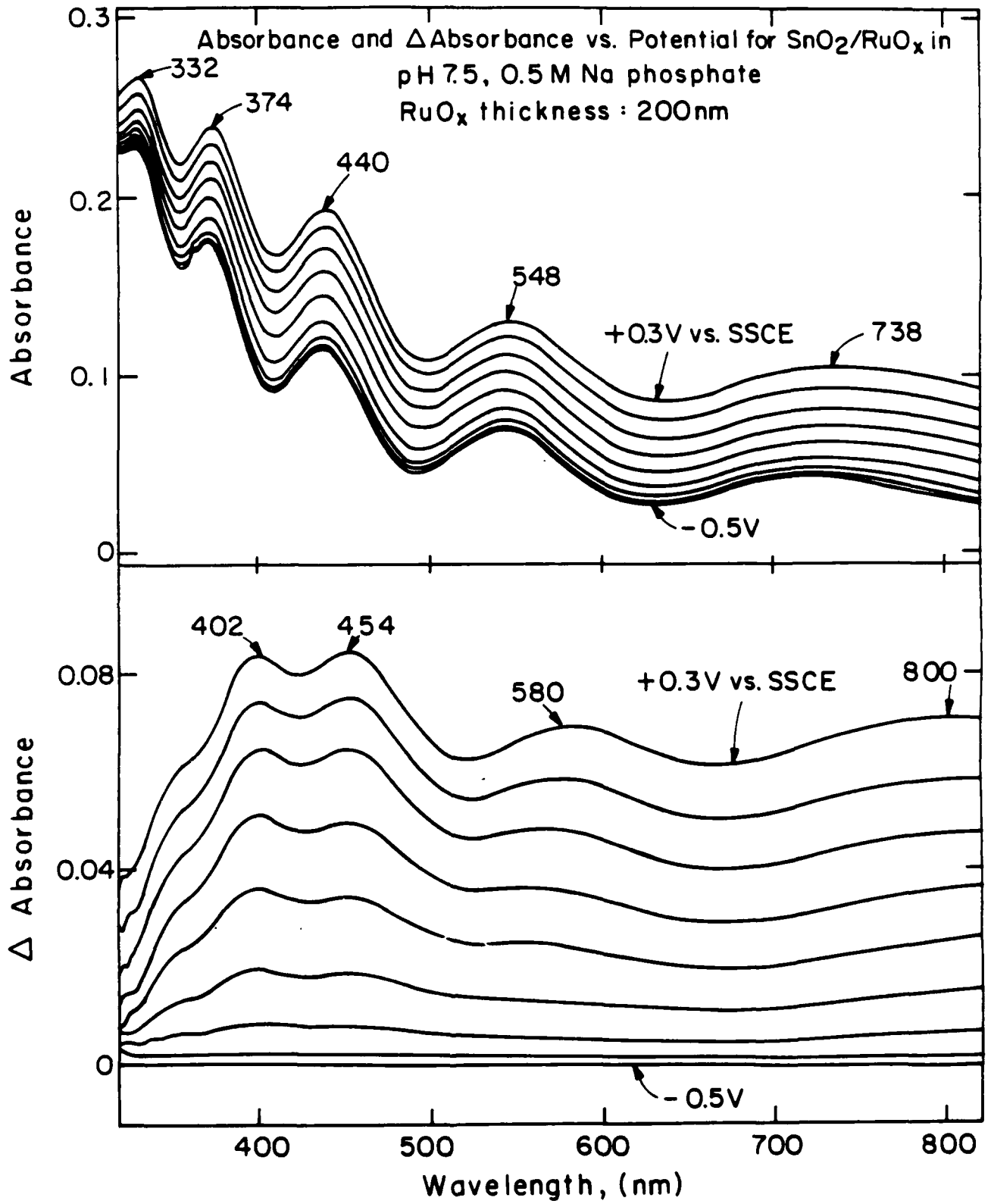
Absorbance and ΔAbsorbance vs. Potential for SnO_2/RuO_x in
pH 7.5, 0.5 M Na phosphate
RuO_x thickness : 200nm
0.3
0.2
0.1
0
Absorbance
332
374
440
548
+0.3V vs. SSCE
738
-0.5V
0.08
0.04
0
Δ Absorbance
402
454
580
+0.3V vs. SSCE
800
-0.5V
400
500
600
700
800
Wavelength, (nm)

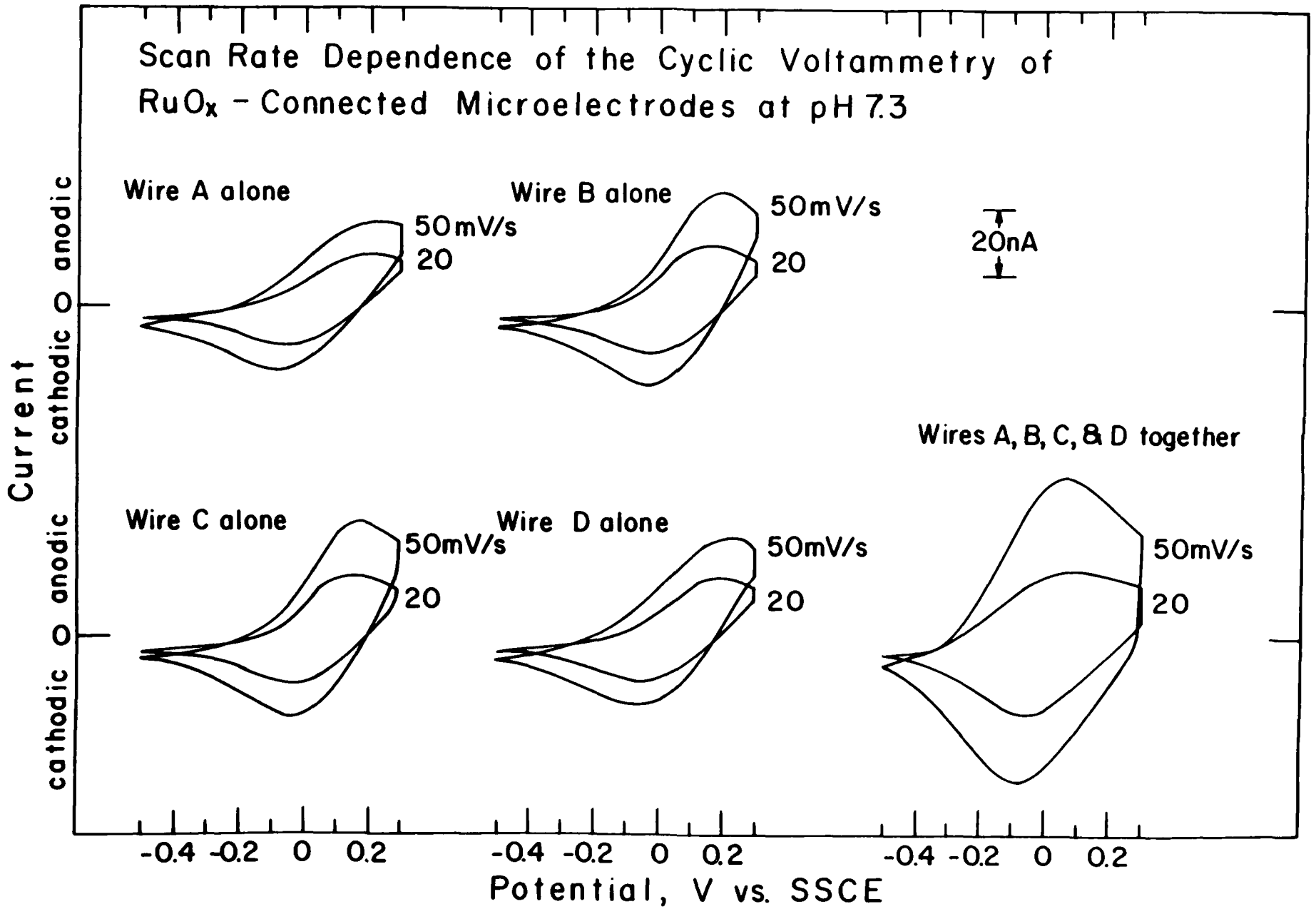
Scan Rate Dependence of the Cyclic Voltammetry of
RuOx - Connected Microelectrodes at pH 7.3
Wire A alone
50mV/s
20
Wire B alone
50mV/s
20
20nA
Wires A, B, C, & D together
50mV/s
20
Wire C alone
50mV/s
20
Wire D alone
50mV/s
20
Current
cathodic O anodic
cathodic O anodic
-0.4 -0.2 0 0.2
-0.4 -0.2 0 0.2
-0.4 -0.2 0 0.2
Potential, V vs. SSCE

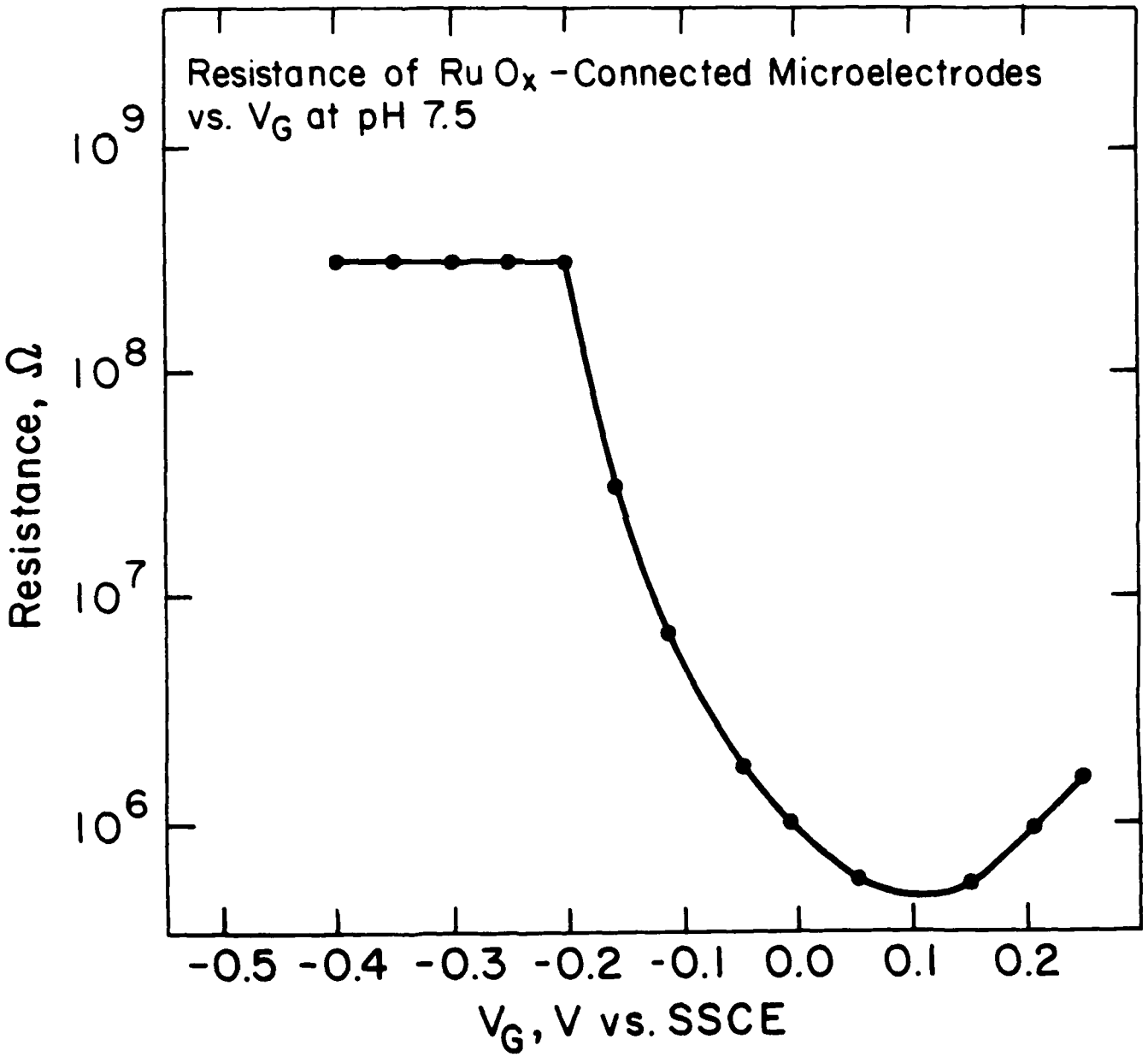
Resistance of Ru O_x - Connected Microelectrodes
vs. V_G at pH 7.5
10^9
10^8
10^7
10^6
Resistance, Ω
-0.5 -0.4 -0.3 -0.2 -0.1 0.0 0.1 0.2
V_G, V vs. SSCE

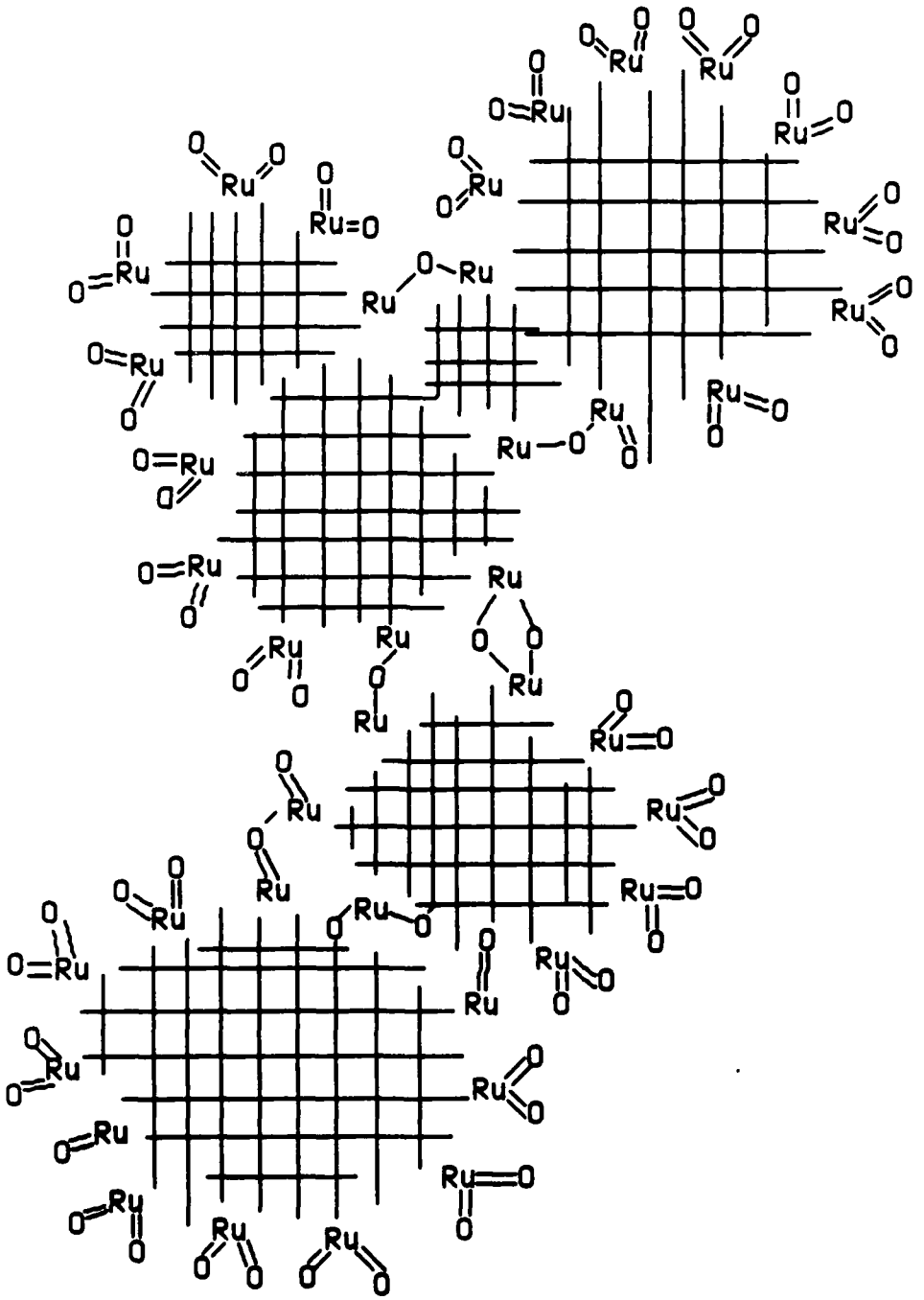
O
Ru
Ru=O

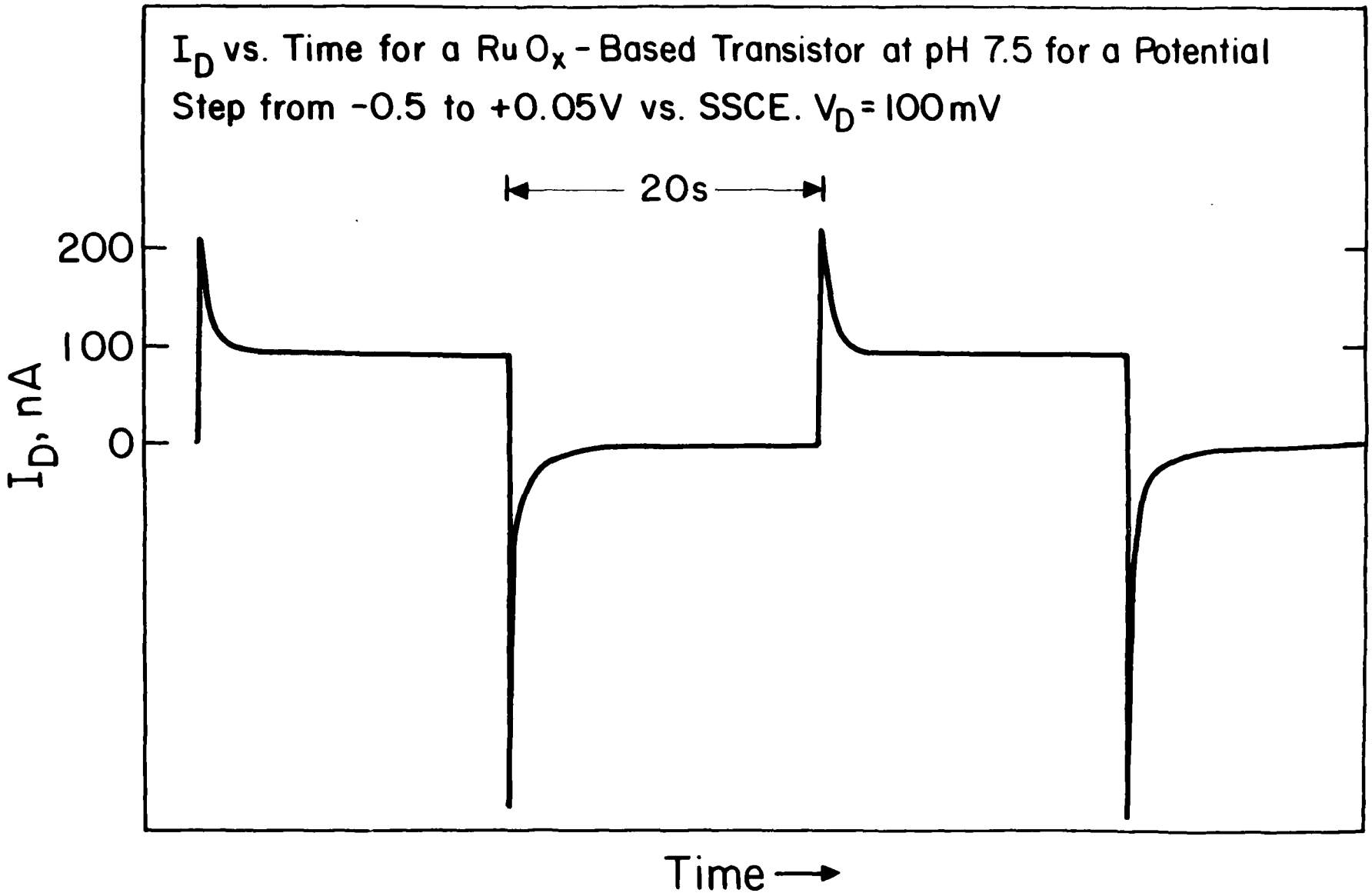
I_D vs. Time for a RuO_x - Based Transistor at pH 7.5 for a Potential Step from -0.5 to +0.05V vs. SSCE. V_D = 100mV
20s
200
100
0
I_D, nA
Time

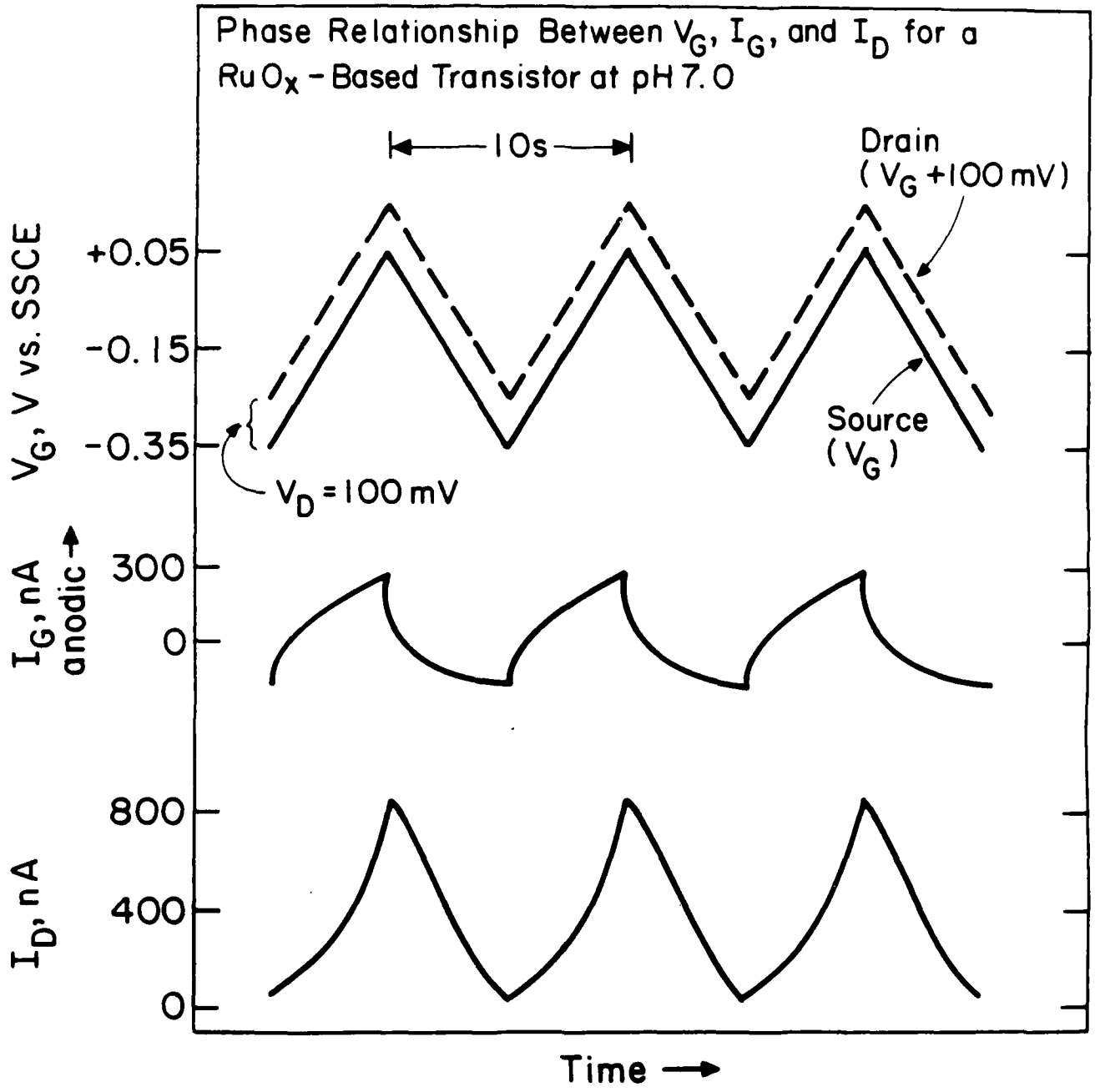
Phase Relationship Between V_G, I_G, and I_D for a RuO_x - Based Transistor at pH 7.0
10s
Drain (V_G +100 mV)
Source (V_G)
V_D = 100 mV
V_G, V vs. SSCE
+0.05
-0.15
-0.35
I_G, nA anodic
300
0
I_D, nA
800
400
0
Time

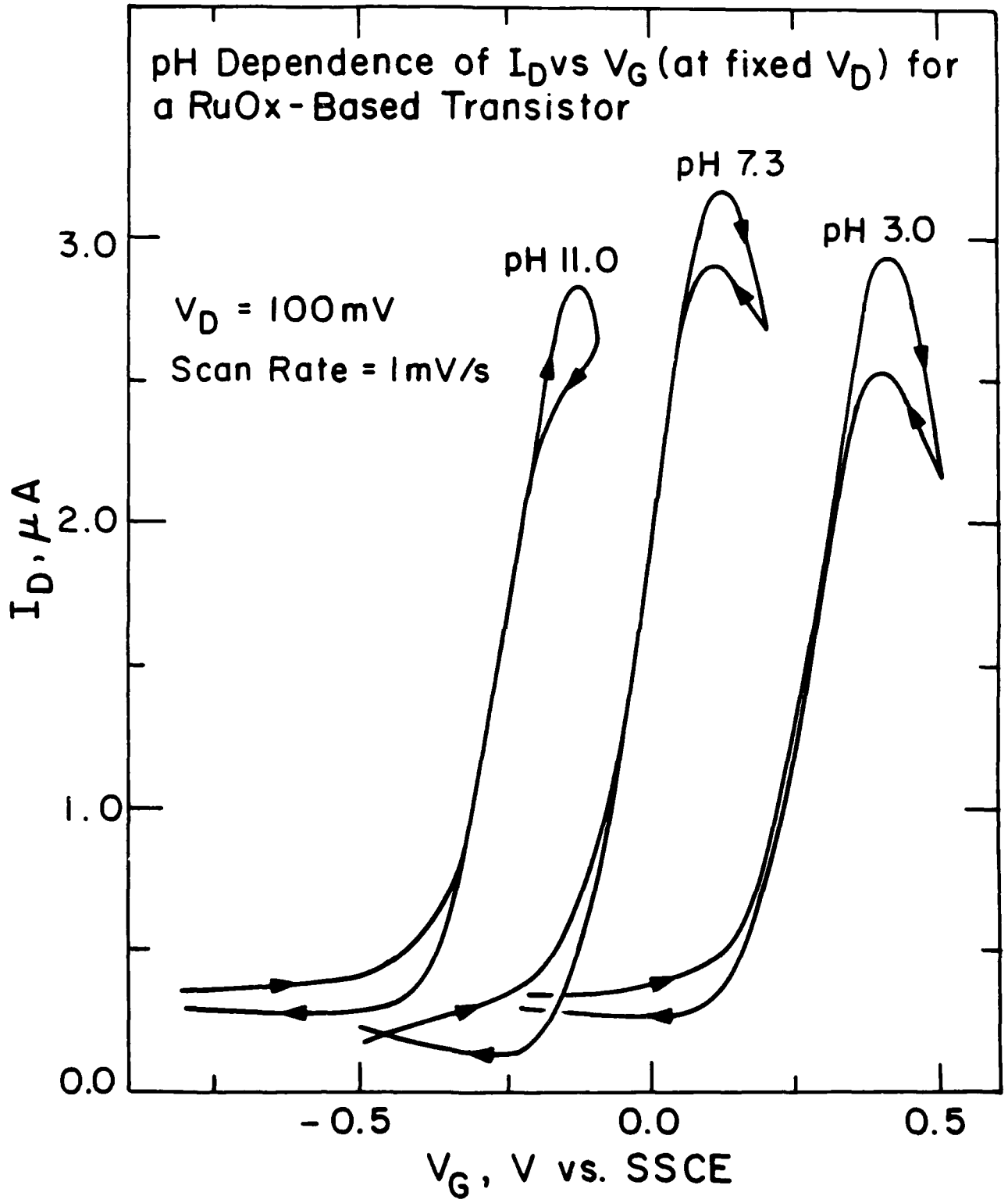
pH Dependence of I_D vs V_G (at fixed V_D) for a RuOx-Based Transistor
pH 7.3
pH 3.0
pH 11.0
V_D = 100mV
Scan Rate = 1mV/s
3.0
2.0
1.0
0.0
I_D, μA
-0.5
0.0
0.5
V_G, V vs. SSCE

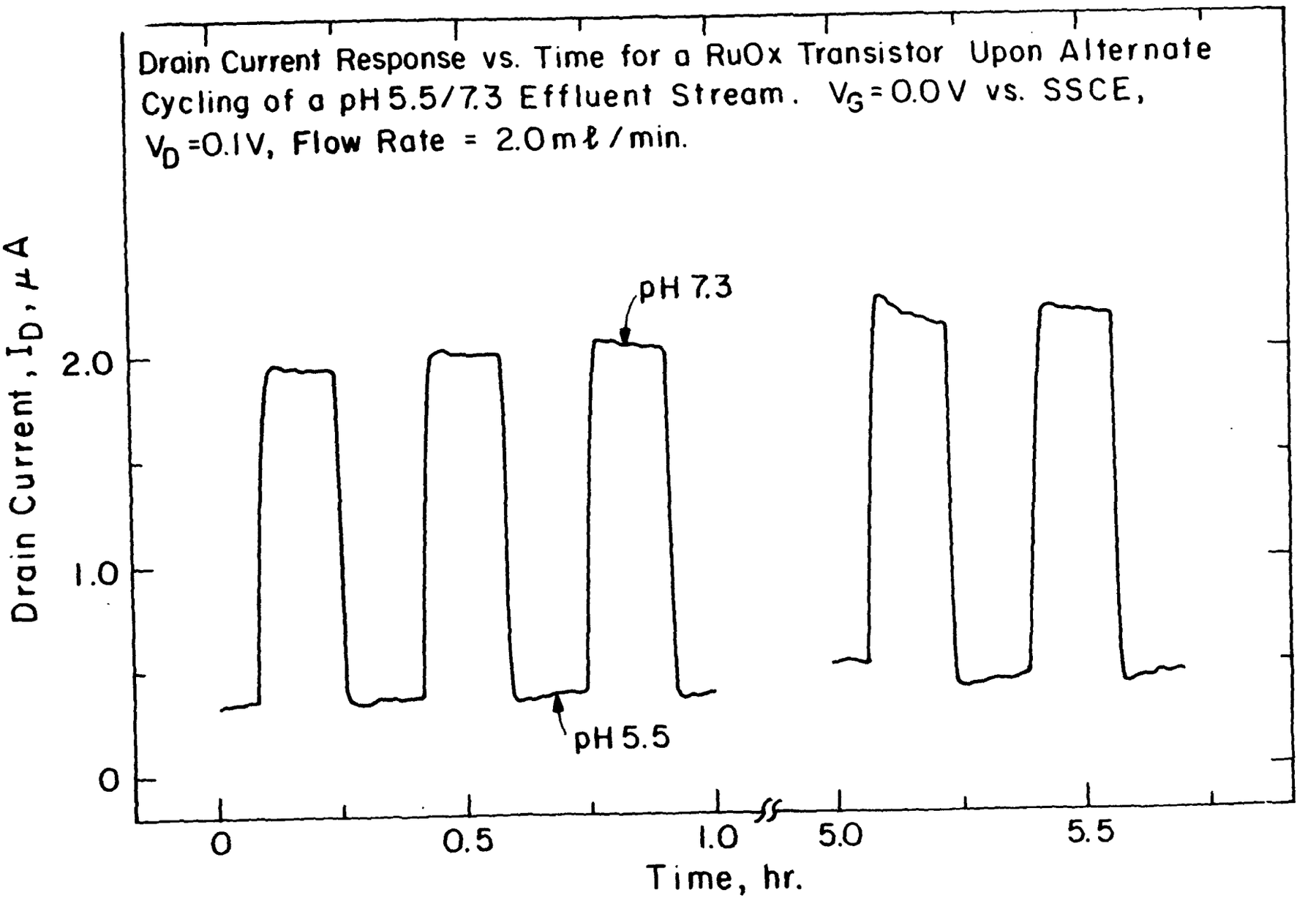
Drain Current Response vs. Time for a RuOx Transistor Upon Alternate Cycling of a pH 5.5/7.3 Effluent Stream. V_S = 0.0 V vs. SSCE, V_D = 0.1 V, Flow Rate = 2.0 mℓ/min.
Drain Current, I_D, μA
2.0
1.0
0
pH 7.3
pH 5.5
0
0.5
1.0
5.0
5.5
Time, hr.

DL/1113/87/2

TECHNICAL REPORT DISTRIBUTION LIST, GEN

	No. Copies
Office of Naval Research Attn: Code 1113 800 N. Quincy Street Arlington, Virginia 22217-5000	2
Dr. Bernard Douda Naval Weapons Support Center Code 50C Crane, Indiana 47522-5050	1
Naval Civil Engineering Laboratory Attn: Dr. R. W. Drisko, Code L52 Port Hueneme, California 93401	1
Defense Technical Information Center Building 5, Cameron Station Alexandria, Virginia 22314	12 high quality
DTNSRDC Attn: Dr. H. Singerman Applied Chemistry Division Annapolis, Maryland 21401	1
Dr. William Tolles Superintendent Chemistry Division, Code 6100 Naval Research Laboratory Washington, D.C. 20375-5000	1
Dr. David Young Code 334 NORDA NSTL, Mississippi 39529	1
Naval Weapons Center Attn: Dr. Ron Atkins Chemistry Division China Lake, California 93555	1
Scientific Advisor Commandant of the Marine Corps Code RD-1 Washington, D.C. 20380	1
U.S. Army Research Office Attn: CRD-AA-IP P.O. Box 12211 Research Triangle Park, NC 27709	1
Mr. John Boyle Materials Branch Naval Ship Engineering Center Philadelphia, Pennsylvania 19112	1
Naval Ocean Systems Center Attn: Dr. S. Yamamoto Marine Sciences Division San Diego, California 91232	1